Version accepted for publication in Ecohydrology 31 March 2020

Turbulence, instream wood and fish: ecohydraulic interactions under field conditions

G. Trinci[1, 2†], G. L. Harvey[1], A. Henshaw[1], W. Betoldi[2], and F. Hölker[3,4]

[1]Queen Mary University of London, Mile End Road, London, E1 4NS, UK.

[2]Department of Civil, Mechanical and Environmental Engineering, University of Trento, Trento, Italy.

[3]Department of Ecohydrology, Leibniz Institute of Freshwater Ecology and Inland Fisheries, Berlin, Germany.

[4]Institute of Biology, Freie Universität Berlin, Berlin, Germany,

Corresponding author: Giuditta Trinci (giuditta.trinci@qmul.ac.uk)

Running head/ short title: Turbulence, instream wood and fish

Abstract

Previous work suggests that ecohydraulics should consider the broad range of parameters that characterize turbulent flow combining Intensity, Periodicity, Orientation and Scale (IPOS; Lacey et al., 2012), but ecohydraulics research under field conditions in natural river systems remains rare, largely due to practical constraints. A novel combination of turbulence properties, computed from high frequency velocity time series, and underwater video of fish habitat use are presented here for two submerged large wood patches on a side channel of the Tagliamento River, Italy, providing insights into ecohydraulic interactions and the first known field application of the IPOS framework. Two adjacent wood patches of similar size reveal distinct differences in turbulence properties and fish habitat use, emphasizing the importance of considering the diverse properties of turbulent flow and reflecting the role of wood structural properties and position in determining the exact nature of hydraulic habitat. Key gradients in turbulence properties derived from multivariate analysis broadly align with IPOS categories, providing statistical validation for the IPOS framework. The application of IPOS to a habitat-focused study demonstrates its utility in understanding and deriving key trends from large and complex turbulence data sets. The results also provide a preliminary indication that IPOS-derived gradients may be helpful in explaining fish habitat selection but these findings need further validation through high spatial resolution studies with different species and bioenergetics models. These insights support previous calls for inclusion of diverse turbulence parameters in ecohydraulics research and, where possible, more explicit consideration of turbulence properties in river assessment, conservation and restoration.

Key Words (max 6):

turbulence; fish habitat; instream wood; woody debris; hydrodynamics

1. Introduction

Turbulent flow is ubiquitous in natural rivers and exerts a fundamental influence on aquatic biota (Vogel, 1994). The turbulent properties of flow generate advantages for aquatic organisms including access to food, locomotion, predator avoidance and waste removal but can also pose threats to critical life history parameters such as survival and growth (Trinci *et al.,* 2017). As a result, turbulent properties represent a fundamental aspect of abiotic river habitats. Despite this, field studies have traditionally focused on the quantification of simpler hydraulic parameters (e.g. mean streamwise velocity), reflecting the difficulties associated with sampling flow velocity at high (turbulent and near-turbulent) frequencies and at scales relevant to individual organisms (Hart *et al.,* 1996; Blanckaert *et al.,* 2013). Notwithstanding these considerable challenges, an improved understanding of hydraulic habitat requirements and use for different aquatic organisms is essential for improving the scientific basis of sustainable river habitat management and restoration (Wilkes *et al.,* 2017). This has led to recent calls for better integration of hydrodynamics into ecohydraulics research (Wilkes *et al.,* 2013) and consideration of the full range of turbulent properties of flow on aquatic organisms (Lacey *et al.,* 2012).

Understanding of the interactions between aquatic organisms and hydrodynamic properties has largely developed through laboratory experimentation using either indoor flumes or outdoor experimental channels, enabling tight experimental control and detailed observation of organism responses at high spatial resolution (Silva *et al.,* 2011, 2012; Goettel *et al.,* 2015; Tullos *et al.,* 2016, Wilkes *et al.,* 2017). While these approaches are attractive in terms of research design and can offer important insights into the bi-directional interactions between organisms and turbulent flow (Cotel and Webb, 2015), laboratory studies have revealed apparently contradictory biotic responses to turbulence properties, partly reflecting variations in experimental design and turbulence parameters considered (see Lacey *et al.,* 2012).

Furthermore, relationships may differ under field conditions due to other environmental factors such as light, temperature and competition (Kemp *et al.,* 2011; Wilkes *et al.,* 2013; Higham *et al.*, 2015). Understanding of the influence of turbulence on fish habitat use in natural streams is limited to a comparatively smaller number of field studies (Cotel *et al.,* 2006), but this is beginning to change. Improvements in the quantification and characterization of turbulence using robust sensors, the increased availability of underwater video cameras, and smartphone technology provide new opportunities for insights into interactions between turbulence and biota in 'real' rivers (Tritico *et al*., 2010; Zhou *et al.,* 2016; Preece, 2017).

Relationships between the 'standard' hydraulic variables (e.g. mean velocity, flow depth) conventionally sampled in habitat assessment studies and turbulent flow properties vary in space and time (Wilcox and Wohl, 2007; MacVicar and Roy, 2007) and hence simpler hydraulic variables cannot be widely used as a proxy for the more complex properties of turbulent flow. Turbulence must therefore be quantified explicitly either by direct measurement of flow velocity at high frequency, flow visualization (e.g. using particle image velocimetry, PIV) or computational fluid dynamics approaches. Turbulent properties can be quantified from high frequency velocity time series through statistical description and the identification of three-dimensional 'eddies' or coherent flow structures (CFS) (Clifford and French, 1993; Lacey *et al.,* 2012; Wilkes *et al.,* 2013). This yields a wide range of parameters that can be used to describe different attributes of turbulent flow. As a result, the range of turbulence parameters selected in previous ecohydraulic research is diverse and highly variable across studies. Lacey *et al.* (2012) synthesized the range of ecologically relevant turbulence parameters that can be computed from high frequency velocity time series into four main categories of turbulence characteristics representing the Intensity, Periodicity, Orientation and Scale of turbulence (the 'IPOS' framework). IPOS provides a novel, practical and ecologically-based framework for studies

exploring the interactions between hydrodynamics and aquatic organisms but is yet to be widely applied in ecohydraulics research (Trinci, 2017).

This paper presents the results of a field experiment investigating the interactions between turbulence and fish habitat use in a natural river channel. The investigation combines low cost underwater videography with the direct quantification of turbulent properties. It represents one of the very few examples of ecohydraulics research under field conditions and provides the first field application of the IPOS framework. Here, we focus on the turbulent flow field generated around instream wood features. Flow obstructions such as large wood and boulders significantly modify local turbulence and can represent important river habitat features (Zika and Peter, 2002; Rifflart *et al.,* 2009; Pilotto *et al.,* 2014). Large wood can provide flow refugia and food sources for aquatic communities, minimise energy expenditure, reduce exposure to predation and increase taxa richness (Schneider and Winemiller, 2008) and is increasingly being used in river restoration design (Wohl, 2017; Cashman *et al.,* 2018; Harvey *et al.,* 2018). The overall aim of the research was to evaluate the utility of IPOS parameters in characterising hydraulic habitat and understanding fish habitat use under field conditions. This is achieved by (i) characterizing the turbulence properties around wood patches; (ii) identifying key trends in turbulence properties and their alignment with the IPOS categories; and (iii) exploring fish habitat use and energy costs and their relationship with IPOS-derived turbulence gradients.

2. Methods

2.1 Field site

The research was conducted in a side channel of the Tagliamento River in Italy (Figure 1) in July 2015. The Tagliamento is one of the last remaining pristine large gravel bed rivers in

Europe (Müller, 1996). Although not completely exempt from human intervention, it is considered to be an important reference system due to its complex physical structure and morphodynamic regime (Tockner *et al.,* 2003). It is braided for much of its course, but the channel narrows and adopts a transitional to meandering style in the lower reaches (Gurnell *et al.,* 2000). The research was carried out on a meandering anabranch of the main channel at Flagogna, 3 km upstream from Pinzano (Figure 1) where, at low flows, a stable hydrological regime is regulated by groundwater (Sukhodolov and Sukhodolova, 2014). In this braided section, the river is highly dynamic and moves freely across a wide (up to 1.5 km) active floodplain, developing a diverse range of morphological features and supporting a unique ecosystem (Ward *et al.,* 1999; Ward and Tockner, 2001). The riparian zone is near-continuous and dominated by two main tree species, *Populus nigra* and *Salix eleagnos* (Karrenberg et al., 2003), which exert a significant influence on morphology and hydraulics (Gurnell et al., 2001; Gurnell and Petts, 2006) through the development of landforms (islands) as well as other wood-related features (exposed tree roots, instream large wood).

The study section was 20 m long and two marginal patches around wood features were selected for survey (Figure 1). Discharge at the time of survey in the side channel was 3.52 $m^3 s^{-1}$, and flow at the upstream main channel gauging station at Venzone was 42 $m^3 s^{-1}$. The first patch (P1) was located on the right bank downstream of a meander bend (Figure 1-C) and was 2.25 m^2 in area with average water depth of 0.57 m. Tree roots and living branches (< 0.15 m diameter and 0.2 – 1.0 m in length) extended into the water from the riparian zone creating a marginal wood feature. The second patch (P2) was on the left bank, 12 m downstream from P1 (Figure 1-C) and was 3.75 m^2 in area with average water depth of 0.53 m. The wood feature combined tree roots from riparian vegetation and trapped submerged small dead wood pieces (wood pieces were 0.06 - 0.15 m diameter and 0.2 - 0.6 m length).

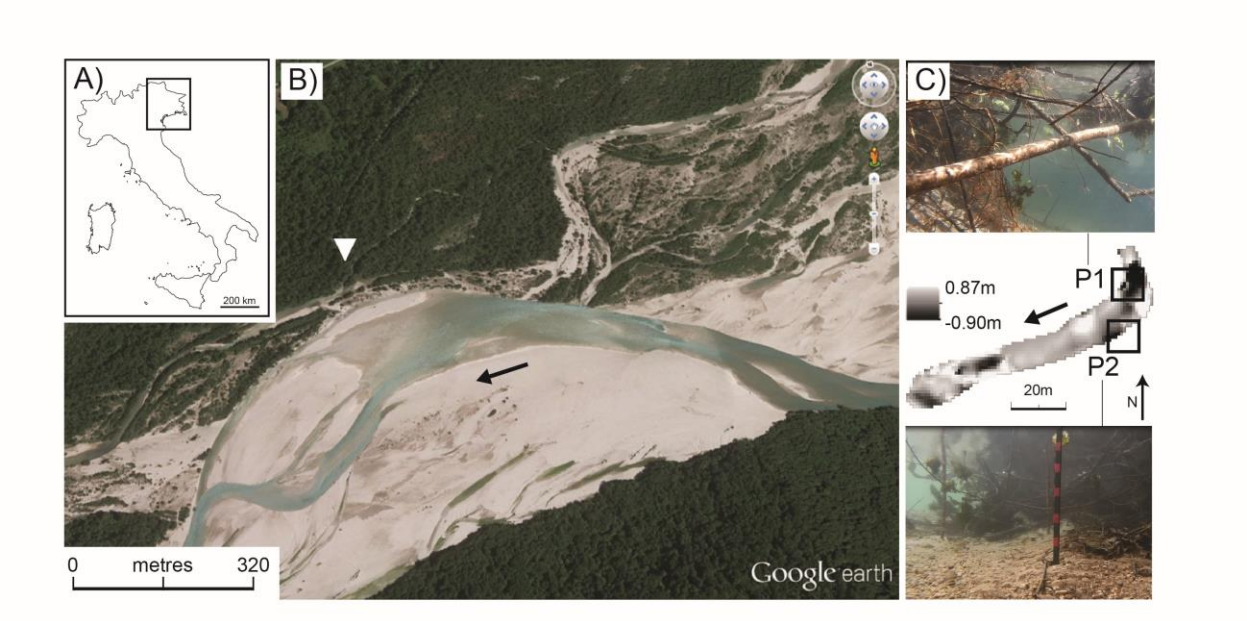

Figure 1: (A) Location of the Tagliamento catchment in Italy; (B) the Flagogna reach showing location of the side channel used for this study; (C) detrended 1 m resolution DEM for the study section showing location of the two patches (P1 and P2; black boxes) with underwater photographs taken of each patch during the surveys.

Fish identified by underwater videography were native European minnow, *Phoxinus phoxinus*, a member of the Cyprinidae family commonly found in freshwater habitats including rivers, ponds and large lakes and noted for shoaling behaviour (Pitcher, 1986; Barber and Wright, 2001). *P. phoxinus* is a slim, small-scaled fish with varied colour from green to brown with small black spots on the back (Mills and Eloranta, 1985). Adults are typically 60-100 mm long, although individuals up to a maximum of 140 mm have been recorded (Ward and Krause, 2001). The diet of *P. phoxinus* includes algae, river plant debris, molluscs, crustaceans and insects (Billard, 1997). They can tolerate water temperature ranges from 4 to 20 ºC (average water temperatures at the time of survey were 15 ºC) and suitable river habitat includes coarse substrate, fast-flowing and well oxygenated water combined with more tranquil pool habitats (Kottelat and Freyhof, 2007), consistent with the characteristics of the study site.

2.2 Topographic and flow data

Topographic surveys were conducted under stable flow conditions using a Leica Total Station T305 in order to provide the topographic context for high frequency flow measurements. The survey was designed to capture bed elevations using a grid of approximately 1 m cell size (Morris *et al.,* 1990), and breaks in slope were used to capture the variation in bed morphology (Brasington *et al.,* 2000). A Detrended Digital Elevation Model (DEM) was created by removing the thalweg and linearly interpolating to a 1 m^2 resolution grid from a Triangulated Irregular Network (TIN; Milne and Sear, 1997; Brasington *et al.,* 2000).

In order to characterise the turbulent properties within each patch, instantaneous velocity measurements were captured at 0.6 of the flow depth (from the water surface) using a Nortek/YSI (Vector) Acoustic Doppler Velocimeter (ADV) within a measurement grid of 0.5 m x 0.5 m. The Nortek Vector measures the 3-dimensional velocities in a small sampling volume with minimal effects on the flow (Nikora and Goring, 1998) using the Doppler effect defined as the change in frequency for a sound wave produced by a moving source. The measurement grid was scaled on the patch size and camera view field for fish observation, yielding 6 within-patch measurements at P1 and 9 within-patch measurements at P2. The Tagliamento is a responsive catchment, which also experiences discharge variability arising from hydropower plants. As a result, a short experimental period of one day was selected in order to ensure measurements were taken under stable flow conditions. Water level was monitored every 10 minutes at an upstream cross section to identify any changes in flow stage. Flow conditions were stable for the duration of the data collection. The spatial resolution of velocity measurements can also influence interpretation of results in habitat use studies (Tullos *et al.,*

2016). Here we selected an intermediate sampling resolution of 0.5 m^2 cells. This resolution is sub-optimal, but higher than the typical spatial resolution for field biology research (1 m^2 – 10 m^2; Leclerc *et al.,* 1995; Tullos *et al.,* 2016) with the aim of reducing errors while capturing adequate spatial coverage within habitat patches and within a short time window of stable flow conditions.

High frequency (32 Hz) flow velocity was recorded in 3 dimensions (streamwise (u), lateral (v), and vertical (w)) at each measurement location for a period of 120 s to accurately capture the majority of macro-scale flow structures in the turbulent/ near-turbulent range (Reynolds number range 10^4 −10^5) (Buffin-Bélanger and Roy, 2005; Hardy *et al.*, 2009; Wilkes *et al.*, 2013). The flow meter was attached to a moveable mounting structure to ensure accurate and stable positioning within the flow field and minimize the degree of flow disturbance (Wilkes *et al.,* 2013).

2.3 Underwater video and derived variables

Underwater videography was used to observe fish presence and swimming behaviour around wood features during the same day in July 2015 in order to ensure stable flow conditions. For each patch, one high resolution (10 MP) underwater camera (Umox SJ4000) was deployed 0.05 m above the river bed, 1 m downstream of each wood feature, between 1.0 and 1.5 m from the bank (Figure 2). Underwater video was captured in 30 minute segments at 3 hour intervals throughout the day between 08.00 and 20.00 and field markers were installed to provide spatial reference points for velocity measurements sampled prior to video recording. The camera can capture images at a rate of 30 frames per second with 32 GB memory and a battery life of 80 minutes, although in practice this was reduced to 40 minutes as a result of relatively low water

temperatures; indeed two 30 minute videos were unfortunately lost due to battery failure (14.00 and 20.00 in P1). In total, we recorded three 30 minutes videos for P1 and five 30 minutes videos for P2. Underwater videography avoids the levels of disturbance introduced by alternative methods such as electrofishing, but a limitation was that we were unable to assess the exact population size in each patch and the fish presence/ absence data may contain repeated observations of the same individuals. This was accounted for where possible in the data analysis (see below).

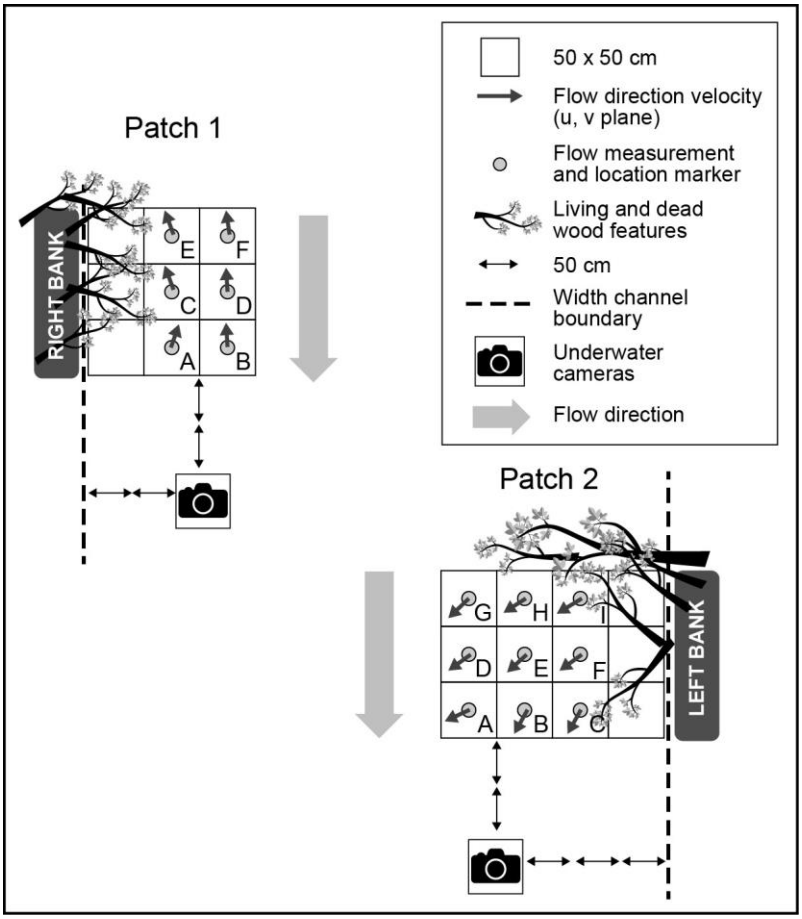

Figure 2. Sampling design for high frequency velocity measurements and instrumentation set up for underwater videography in the two wood patches. Grey arrows show the resultant velocity derived from u (streamwise) and v (cross stream) component at each point.

Recent advances in video processing systems provide rapid, automated techniques for identifying, counting and tracking movements of fish (Spampinato *et al.,* 2010; Delcourt *et al.,* 2013; Dell *et al.,* 2014; Neuswanger *et al.,* 2016). However, since the videos were captured under field conditions, a range of factors including luminosity, turbulence, air bubbles, water turbidity and movement of the wood features within the flow limited the use of auto-tracking software in this study. Instead, videos were observed manually at 60 s intervals (generating 90 instantaneous observations for P1 and 180 for P2) in order to record fish abundance, length, position and movements in relation to the velocity measurement grid, using instream markers.

For each video observation, the selection index (SI) was used to quantify the proportion of fish in each location of the patch by calculating the number of time a fish was observed in the area around the measurement (CO_{cell} = Σ fish in each cell) over the maximum cell occupancy (CO_{max}) (Wilkes *et al.,* 2017) as shown in Equation 1.

$$SI = CO_{cell} / CO_{max} \quad \text{Eq. (1)}$$

Fish behaviour was assigned to one of two activities observed during the period of record: 1) station holding, where fish maintained the same position in the flow for 10 s or more and 2) foraging activity where fish crossed one or more cells in the measurement grid. Station holding is usually associated with energy conservation and predator avoidance while foraging activity reflected a feeding strategy (Webb, 1988). Fish swimming speed was estimated for the two different behaviours by considering two swimming patterns: (i) forced swimming defined as swimming against the prevailing flow direction and (ii) spontaneous (directed) swimming defined as a straight line movement from one location to another (Boisclair and Tang, 1993). For station holding behaviour, swimming speed was represented by forced swimming (i.e. local flow

velocity). For foraging behaviour, swimming speed was estimated as the sum of forced swimming speed (using the resultant velocity and flow direction derived from streamwise and lateral velocity components at the destination point) and directed swimming speed (distance moved in a given time period).

To quantify the influence of turbulence on fish energy expenditure, a bioenergetic model was applied to calculate the total swimming cost (SC) defined as the sum of the energy required by the animal for external movements and the standard metabolic rate. The two turbulent SC models (SC_1 and SC_2) consider the effects of hydrodynamic variables (mean velocity, streamwise turbulence intensity and Turbulent Kinetic Energy (TKE)) together with fish body mass and water temperature (Equation 3 and 4) to evaluate the overall energy expenditure (Enders *et al.,* 2005). This approach provides a valid alternative to the direct measurement of energy costs (e.g. by using respirometer experiments) that requires tightly controlled laboratory conditions (Enders *et al.,* 2016). There is no existing bioenergetics model for *P. phoxinus*, hence a model originally parametrised for Atlantic salmon, *Salmo salar*, was applied. *S. salar* is a streamlined fish with a similar morphology to *P. phoxinus*. This approach is used frequently in bioenergetics, but can result in inaccuracies in metabolic rates even in closely related species (Enders *et al.,* 2005; Enders and Scruton, 2006; Enders, pers. comm). Fish body mass (M; measured in g) was estimated by mass-length equations (Equation 2) for *P. phoxinus* (Oscoz et al., 2005) using observed fish body length, L (cm) (Froese, 1998; Miranda *et al.,* 2006).

$$M = 0.0042 * L^{3.4210} \qquad \text{Eq. (2)}$$

$$\log SC_1 = 0.23 \log T + 0.64 \log M + 2.43 \log U + 0.67 \log u_{sd} - 4.06 \qquad \text{Eq. (3)}$$

$$\log SC_2 = 0.23 \log T + 0.62 \log M + 0.44 \log TKE - 1.21 \quad \text{Eq. (4)}$$

(SC: total swimming cost (mg O^2 h^{-1}), T: water temperature (°C), M: fish body mass (g), U: mean flow velocity (cm s^{-1}), u_{sd}: turbulence intensity on u component (cm s^{-1}), TKE: turbulent kinetic energy (cm^2 s^{-2}))

A dimensionless metric (external to the IPOS framework) expressing the ratio of eddy length to fish body length (length ratio; LR) has also been proposed as an important parameter in assessing the impacts of turbulence on fish (Cotel and Webb, 2015). This is defined by Equation 5, where L_e is the average eddy size and F_L is the fish body length.

$$LR = L_e / F_L \quad \text{Eq. (5)}$$

2.4 Data processing and analysis

To ensure quality control, visual observation of time series plots was used to explore velocity variability and identify possible spikes (Chatfield, 2004). WinADV (version 2.028) (US Bureau of Reclamation) was used to filter the velocity data for noise (spikes) using the Signal to Noise Ratio (SNR > 20) and correlation (COR > 70%) parameters (Goring and Nikora, 2002; Rusello *et al.,* 2006). Stationarity tests were performed for each time series and non-stationary time series were detrended using linear or second order regression as appropriate (Clifford, 1993; Harvey and Clifford, 2009). Following visual inspections and stationarity checks, all time series met the data quality requirements and were retained for analysis. To quantify turbulence in both

patches, 13 variables from across the four IPOS categories were then computed as outlined in Trinci *et al.* (2017) for each point measurement (see Table 1).

Data were not normally distributed (Shapiro - Wilk: $p < 0.001$) and therefore non-parametric statistical tests were used. Multivariate statistical analysis (Principal Components Analysis; PCA) was used to identify the key gradients in turbulence properties within the data sets. Prior to PCA, Kaiser-Meyer-Olkin (KMO) and Barlett's test of Sphericity were analysed to identify redundant variables and check correlations between variables respectively. A group of thirteen hydrodynamic variables were retained for the PCA analysis and include: relative intensity on the u and w components (TIu and TIw), turbulent kinetic energy (TKE), kurtosis on the u and w components, skewness of the turbulent residuals on the u and w components, pseudo-periodicity on the w component, spatial eddy scale on the u and w directions (Lu and Lw), together with magnitude of flow event structure derived from quadrant analysis ((ejections (Q2) and inrushes (Q4)). A Generalised Linear Model (GLM) was used to predict the selection index by fish using overall velocity, SC_1, SC_2 and PCs that reflect a combination of hydrodynamic variables (PC1, PC2, PC3) as well as the resultant flow velocity for comparison. A repeated measures test (Wilks-Lambda) was performed to account for the fact that fish observation data could include the repeat-counting of the same individuals at different time periods. Results confirmed the different time periods could be treated as independent samples for the purposes of the GLM ($p < 0.05$). Data followed the Poisson distribution ($p > 0.05$) but the overdispersion test that evaluates the degree of data variability (Dean, 1992) revealed a high dispersion rate (variance >> mean) only for SC_2 that was removed from the analysis. A Poisson regression model was then applied to the other variables listed. To compare the goodness of fit and the performance of each model, we used Akaike's Information Criterion (AIC) and the Bayesian

Information Criterion (BIC). All analysis were performed in either XLSTAT Base Microsoft 2018, SPSS v22 and Matlab R2018b.

3. Results

3.1 IPOS characteristics of the wood patches

P1 was characterized by rotational flow, with negative streamwise velocities indicating flow in the upstream direction at all measurement locations (mean -0.11 ms^{-1}). In contrast, P2 was characterised by positive streamwise velocity indicating the main direction of flow was downstream (mean 0.18 ms^{-1}). Lateral flow velocities in P2 indicated preferential flow deflection towards central channel areas for both patches (Figure 2). The mean velocity (u and v components) was significantly different between the patches (Mann Whitney $p < 0.05$). As shown in Table 2, P1 was associated with higher Reynolds stresses and TKE, lower vorticity, a less predictable flow structure and a tendency for higher magnitude ejections (Q2) and inrushes (Q4) compared to P2. Eddy length and diameter were similar between the patches but with slightly higher average dimensions for the streamwise dimension in P2. The two patches therefore revealed minor differences in their high frequency flow properties, but only the magnitude of outwards interactions and pseudo-periodicity on the w component were statistically significant between the patches (Mann Whitney U, $p < 0.05$). The majority of velocity time series in P2 met the condition for pseudo-periodicity, indicating a more predictable flow structure, while the majority of series for P1 did not meet the condition.

The spatial organization of selected IPOS flow properties in P1 and P2 is explored in Figure 3 to illustrate the notable trends. For P1, within-patch variability broadly followed an upstream to downstream gradient, with higher TKE and Reynolds shear stress values and smaller eddy

lengths (Lu component) in the upstream part of the patch relative to the downstream zone. The relative contributions of the four event quadrants were highly variable in space, but in the majority of measurement locations, one or two quadrants were dominant. For P2, TKE and Reynolds shear stress values were greatest in the outer flow and lowest in the intermediate zone between the wood and the outer flow. Eddy lengths (Lu component) were greatest close to the wood and in the downstream zone of the patch. Again, there is a tendency for one or two event types to dominate across the majority of measurement locations but with considerable variability in the dominant event type.

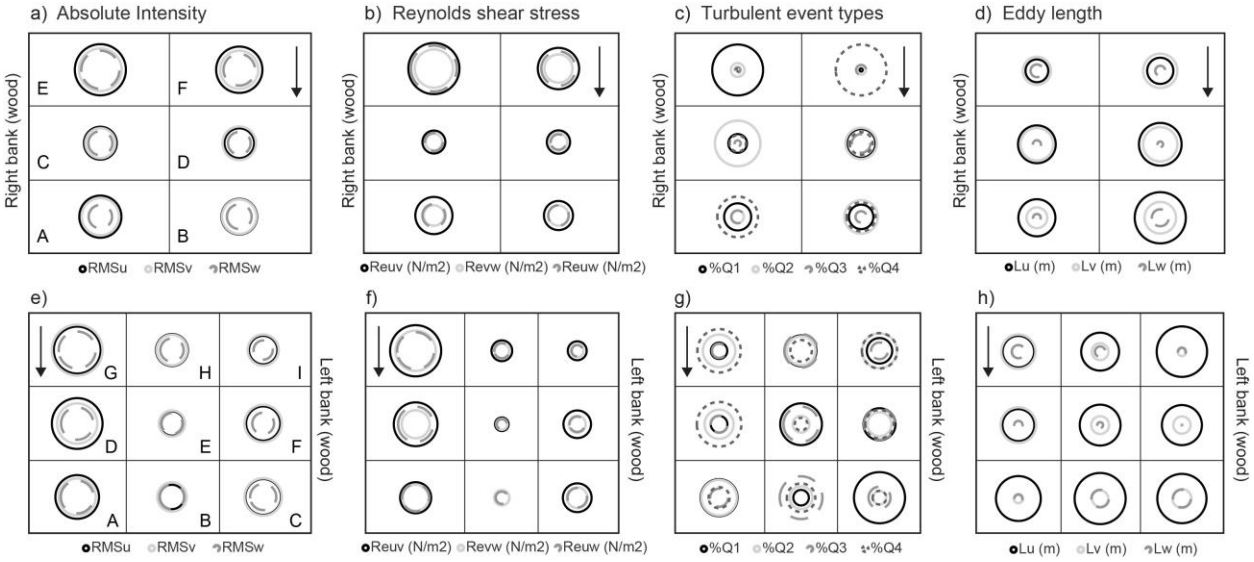

Figure 3. Spatial organisation of key turbulence properties for the two wood patches – P1 (a-d) and P2 (e-h). Moving from left to right, the plots show results for absolute turbulent intensity, Reynolds shear stress, events types derived from quadrant analysis and eddy length scales. Columns represent the cross stream dimension, showing measurements taken near the wood and in the outer flow. Rows represent the upstream - downstream dimension. Size of circle denotes magnitude of variable. Black arrows show the flow direction.

PCA revealed four PCs with eigenvalues greater than 1, but analysis focused on the first 3 PCs, which had clearer physical meaning and cumulatively explained 73% of the variance in the data.

PC1 was characterized by high variable loadings for turbulence intensity metrics (u'w' = 0.898, u'v' = 0.885 and Tiu = 0.795) and was interpreted to reflect an 'Intensity' gradient. PC2 was characterized by high variable loadings for eddy size (Lu = 0.802) and event structure (Q2 = -0.651) in addition to intensity in the w dimension (Tiw = 0.881) and was interpreted to reflect 'scale and orientation'. PC3 was characterized by the periodicity variable of kurtosis on u component in addition to vertical intensity and was interpreted to represent 'periodicity'. Upstream-downstream variation is more apparent for P1 (PC3) and lateral variation from the wood to the outer flow is more apparent for P2 (PC3 and, to a lesser extent PC1) but there is high within-patch heterogeneity for both patches across the PCs (Figure 4).

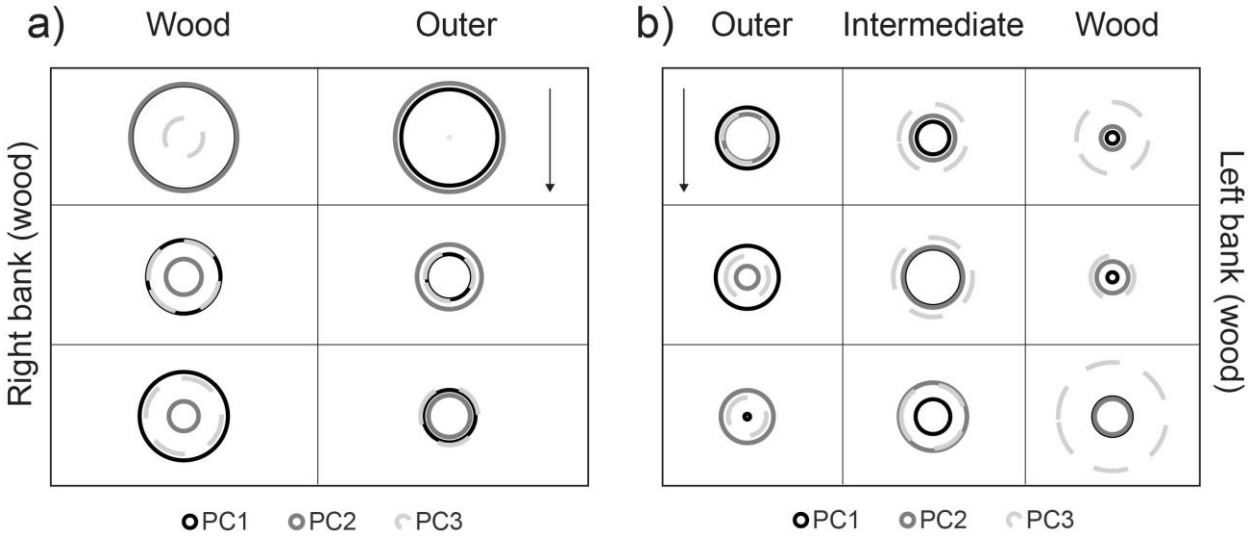

Figure 4. Spatial organisation of principal components across Patch 1 (a) and Patch 2 (b) for PC1 (turbulence intensity), PC2 (scale and orientation) and PC3 (periodicity). PC3 was statistically different between wood and outer points in both patches. Columns represent the cross stream dimension, showing measurements taken near the wood and in the outer flow. Rows represent the upstream - downstream dimension. Size of circle denotes magnitude of PC scores. Black arrows show the flow direction.

3.2 Habitat use and swimming costs of *P. phoxinus* in the two patches

The abundance and average length of fish occupying areas within the two patches through the sampling period is presented in Figure 5a and 5b. The average number of fish observed in each video ranged between 11 and 18 for P1 and between 1 and 11 for P2. *P. phoxinus* were more abundant (mean abundance 12 individuals) and individuals were smaller (mean 4 cm) in P1 compared to P2 (mean abundance 4 individuals; average length 8 cm). Fish length did not vary considerably through the day in P1, while in P2 size increases through the day before decreasing immediately before sunset. Both activities (foraging and station holding) were observed in each patch (Figure 5c and 5d), but station holding was more frequently observed in P2 (60.5% of total observations) while foraging was more frequently observed in P1 (67% of total observations). The diurnal trends show station holding accounted for > 50% of observed activity for all but one time period in P2 (14.00), and foraging accounted for > 50% of observed activity at two of the three time periods in P1 (11.00 and 17.00). Estimated mean swimming speed (Figure 5e and 5f) for station holding activity ranged between 9 cm s^{-1} and 27 cm s^{-1} (mean 13 cm s^{-1}; based on forced swimming estimates) while estimated mean swimming speeds for foraging activity ranged between 13 cm s^{-1} and 23 cm s^{-1} (mean 18 cm s^{-1}; based on directed swimming estimates). Swimming speeds for each activity type were similar among the two patches, with the exception of station holding in P1, which was lower for the 08.00 and 11.00 time periods. The selection index (Figure 6) was higher in P1 compared to P2. The intermediate/wood areas were higher compared to outer areas in both patches. In addition, the index was zero for outer zones in P2.

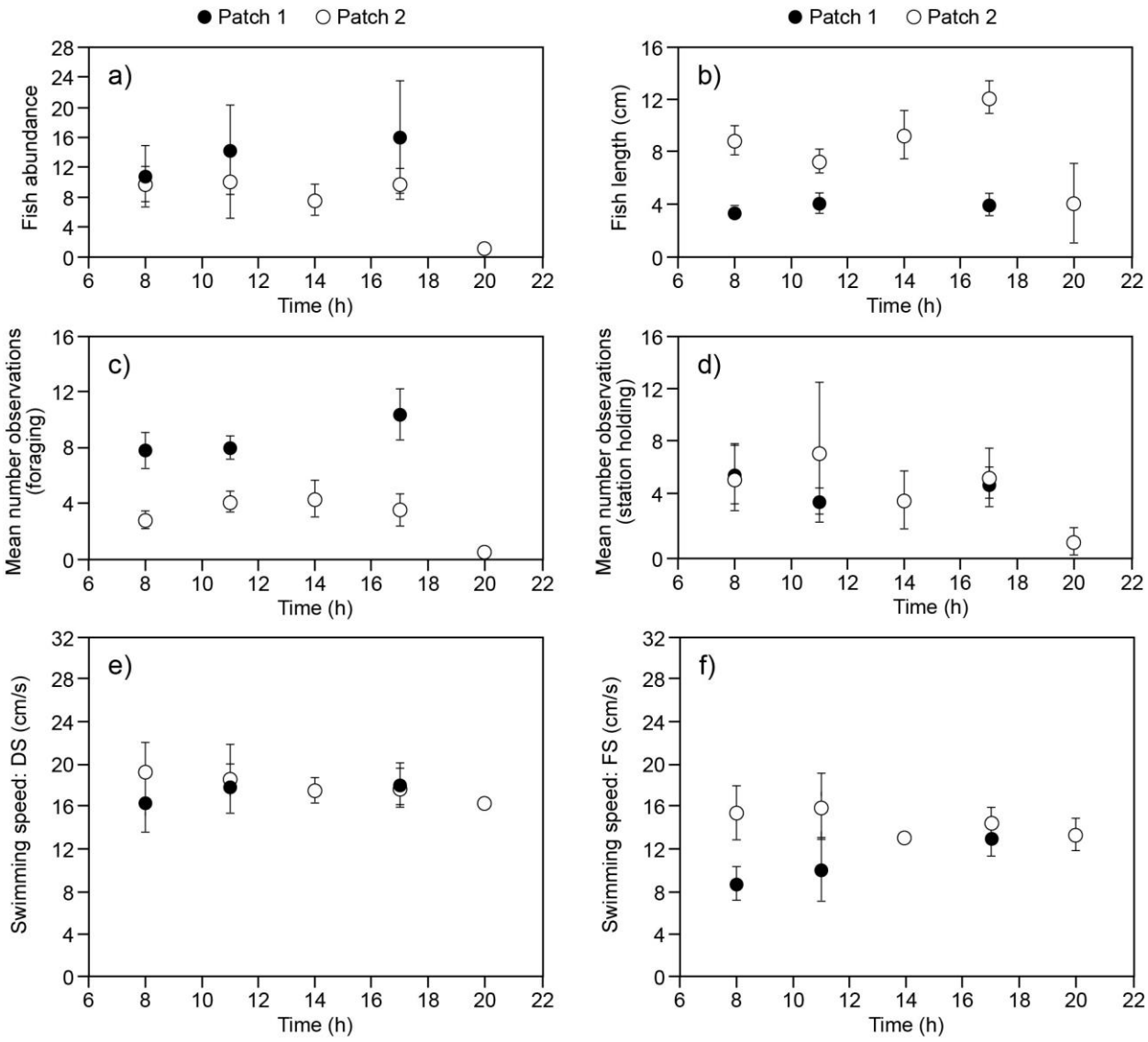

Figure 5 Fish related variables for the two wood patches (P1 = black circles; P2 = white circles) through the underwater video survey period: (a) Fish abundance (b) fish body length, (c) mean number of observations of foraging activity, (d) mean number of observations of station holding activity, (e) directed swimming speed (DS), (f) forced swimming speed (FS).

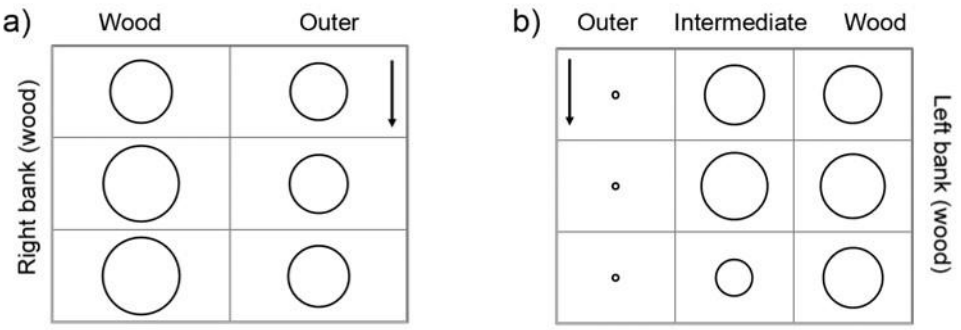

Figure 6. Fish habitat selection index (SI) for the two patches. Results are organised by patch. Columns represent the cross stream dimension, showing measurements taken near the wood and in the outer flow. Rows represent the upstream - downstream dimension. Size of circle denotes magnitude of PC scores. Black arrows show the flow direction.

In both patches, the total swimming cost was estimated using two turbulent bioenergetic models (see equations 3 and 4) to quantify the energy expenditure of small (average length 4 cm) and large (average length 8 cm) fish in P1 and P2, respectively. Model SC_1 used mean velocity and standard deviation on the u component to predict the total swimming cost while model SC_2 used turbulent kinetic energy as the descriptor of turbulence to compute the swimming cost. Both models predicted higher swimming costs for P2 compared to P1 (Figure 7 a and b), but a greater difference between patches was observed overall for the SC_2 model. Swimming costs did not vary spatially within P1, but for P2 higher swimming costs were associated with outer flow zone and lower swimming costs with the areas closer to the wood. Figure 7c shows the ratio between eddy length scale and fish length for the two patches. For P1, ratios are greater than 1, indicating eddy length scales exceeded fish body length, while ratios are mostly less than 1 for P2 where fish were larger in length. Values closer to 1, indicating potential for eddies to have a destabilizing effect on fish, are more apparent in P2, but the majority of locations in both patches do not have ratios close to 1.

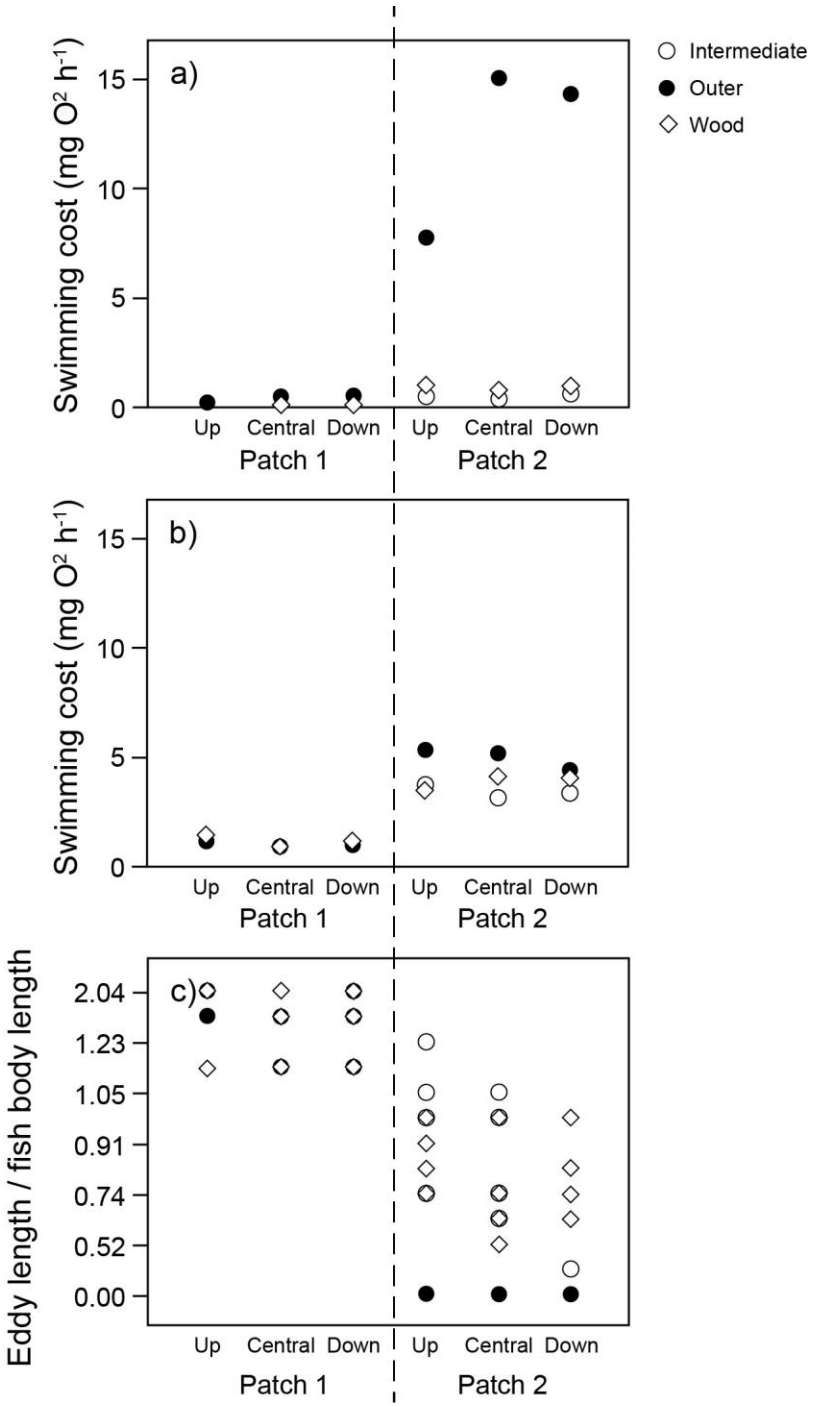

Figure 7. (a) Predicted swimming cost using absolute intensity (Eq.3); (b) predicted swimming cost using turbulent kinetic energy (Eq. 4); and (c) eddy length: fish ratio for each observation. Results are organised by patch and distance downstream on the x-axis. Symbols denote cross stream position of measurement location (beside the wood feature, in the intermediate area, or in the outer flow).

Generalized linear models (GLMs) were run using the resultant velocity, SC and the three PCs. The model was statistically significant (X^2 = 338.13, p <0.0001) (Table 3) and the AIC and BIC values were positive (AIC = 140, BIC = 129). The models for SC_1, PC1 (intensity) and PC3 ('periodicity') were statistically significant, indicating that these variables are most helpful in explaining fish habitat selection. The relationships suggest *P. phoxinus* preferences for areas of lower turbulence intensity, smaller eddy sizes and lower magnitude turbulent 'events' and kurtosis in the turbulent residuals.

4. Discussion

Spatial organization of individual turbulence properties was complex, but multivariate analysis derived key gradients in turbulence properties that were linked to the IPOS categories: intensity, scale and orientation, and periodicity. This provides support for the utility of the IPOS approach and underlines the importance of exploring a range of different characteristics of turbulent flow in ecohydraulic applications. Importantly, these gradients, and in particular the flow intensity and periodicity gradients, alongside the SC_1 swimming costs model were most helpful in explaining fish habitat selection. The approach used here therefore provides a practical response to the call for consideration of a more comprehensive range of turbulence properties in relation to hydraulic habitat (Lacey *et al.,* 2012; Wilkes *et al.,* 2013). A limitation of the study is lack of velocity measurements at multiple vertical positions within the flow field, and the focus on a single flow stage. Further studies could incorporate vertical variation, in addition to streamwise and cross stream measurement of turbulence, and explore dynamics with stage. This would be time and labour intensive and more challenging from a practical perspective but adaptation of laboratory techniques for field use, such as Particle Imaging Velocimetry may assist here (Trinci *et al.,* 2017).

Assessment of a range of turbulence properties within the IPOS framework also revealed differences in the hydraulic habitat provided by the two wood features. P1 was located downstream of a meander bend characterised by rotational flow and exhibited evidence of higher flow intensity and less predictable flow structure compared to P2, which was located in a straight section of channel. Both patches were characterized by high levels of internal variability in turbulence properties but with differences in spatial organization of flow characteristics. There was a broad trend for hydraulic variability in the longitudinal dimension in P1, with greater turbulence intensity and a less predictable flow structure in upstream areas, which may reflect the effects of secondary circulations at the bend (Hooke, 1975; MacVicar and Roy, 2007; Blanckaert *et al.,* 2009). Cross stream variability was more pronounced in P2 where the wood feature diverted the water flow to the central part of the channel, developing sheltered areas of lower shear stress and kinetic energy at the margins and higher turbulence intensity zones in central channel areas. These findings contrast with Tullos and Walter (2015) who found higher intensity turbulence nearer the wood features, emphasizing that the hydraulic effects of the wood features reflect the size and structural properties of the wood as well as its position within the channel.

Different habitats may be used by fish for different activities (e.g. feeding, resting, predator avoidance, exploring) and habitat selection varies with the size (life stage) of the fish in combination with physical conditions such as flow velocity (Tiffan *et al.,* 2010). *P. phoxinus* were observed in both patches throughout the day, but fish were more abundant and smaller in P1 Differences in body length across the two patches may reflect patch occupation by fish of different life stages. Specifically, P1 nose to tail body average lengths (40 mm) correspond broadly with belly length of juvenile minnows (27 - 57 mm) and P2 (83 mm) with adult minnows

(belly length > 57 mm) as reported for lowland rivers (Simonovic et al., 1999). Foraging activity was more common in P1, while station holding was more common in P2. This corresponds with observation of swimming modes that facilitate food intake among juveniles (Griffiths, 1997).

Fish abundance was highest in areas near the wood and in the downstream sections that were also characterized by low/medium shear stress and turbulence intensity on the vertical component. Station holding behaviour was generally observed in areas close to the wood, and foraging behaviour in areas further from the wood/outer flow in P1. Eddy length: fish length ratios in these areas were also not close to 1. This is consistent with previous experiments using Iberian barbel (Silva *et al.,* 2012), which indicated that fish spent more time in areas with lower turbulence intensity and in areas with eddies that are either larger or smaller than their body length. Tritico and Cotel (2010) used laboratory experiments to demonstrate how eddy size influenced the stability system of fish, reducing their body control and causing individuals to lose their swimming trajectories. The dimensionless length scale ratio that compares fish body length and characteristic eddy length scale has therefore been proposed as a key influence on fish behaviour and stability (Cotel and Webb, 2015).

The presence and activity of *P. phoxinus* around wood features is likely to reflect a range of habitat functions provided by instream wood, including cover, temperature moderation and food resources (Cui and Wootton, 1988; Plath *et al.,* 2013). Estimated total swimming costs, however, can provide insights into relationships between energy expenditure and habitat selection, which will reflect the hydraulic environment. Larger fish expend more energy, although increased energy costs are not directly proportional to length as a result of gains in swimming efficiency (Webb *et al.,* 1984; Fish, 2010). In this study, the SC_2 model (which incorporates TKE) revealed much higher values for P2 compared to P1 while the SC_1 model

(which uses streamwise turbulence intensity only) produced similar values between the two patches, with the exception of the outer flow in P2. The results of the fish bioenergetics models were comparable with previous studies (Enders *et al.,* 2003; Wilkes *et al.,* 2017). However, the results here are treated as preliminary for several reasons. The model was developed for juvenile Atlantic salmon in an experimental laboratory. Model outcomes may therefore be influenced by variables such as fish length, life stage and photoperiod (Enders and Scruton 2006; Tiffan *et al.,* 2010; Benitez and Ovido, 2018) in addition to the spatial resolution of velocity measurements (Tullos *et al.,* 2016). A limitation associated with the underwater videography approach is the potential for repeat observations of the same individual. While this was accounted for by using a repeated measures analysis, repeated observations can introduce 'order effects' that arise from exposing fish to multiple patches.

The research also highlights some challenges and opportunities for future research. Practical constraints often mean that ecohydraulics research cannot span the range of scales in hydrodynamic properties relevant to organisms at a particular location in the river channel. For example, in this study although a wide range of turbulence properties were explored, secondary circulations and microscale viscosity processes were not considered, and vertical variation in turbulence through the water column or variations with flow stage were not captured. Underwater videography was successfully used here to provide observational data on fish habitat use, but the technique is associated with numerous challenges when applied in the field. While the method is not associated with harmful effects, it can be intrusive with potential for influencing animal behaviour (Spampinato *et al.,* 2008). Use of tracking systems to identify fish location and/or simultaneous deployment of multiple cameras would provide more detailed locational information on fish and avoid repeated observations of the same individuals (Tullos and Walter, 2015). A further challenge is the laborious nature of post-processing of video files if

approached manually. Recent advances in auto-tracking software can help to capture detailed information of fish under controlled laboratory conditions (Dell *et al.*, 2014; Tullos and Walter, 2015). The accuracy and reliability of these methods when applied in river environments, however, is currently limited by the complexity of the flow field, which may include many moving elements that are difficult to distinguish using existing automated methods.

5. Conclusions

This paper presents a novel methodological approach combining underwater video and turbulence measurement under field conditions. The approach may be explored more widely in further research, offering new insight into fish behaviour and habitat use. The study also presents the first application of the IPOS framework and provides statistical validation of the intensity, periodicity, orientation and scale categories as key gradients in turbulence properties. The work demonstrates the utility of IPOS in guiding study design and deriving trends from complex turbulence data sets and provides a response to calls within the literature for better consideration of a diverse range of turbulence characteristics in ecohydraulics research. By applying an existing bioenergetics model to *P. phoxinus* the results also provide a preliminary indication that IPOS-derived gradients may be helpful in explaining fish habitat selection. These findings need further validation through studies with different fish species and associated customised bioenergetics models, and with higher spatial resolution of turbulence measurements. Further research may also explore if variations in wood-turbulence-fish interactions vary with flow stage, species and life stage. In addition, there were marked differences in the spatial organisation of turbulence properties and fish habitat use (abundance, size, behaviour) between two closely spaced but differently structured and positioned wood patches. Instream wood is increasingly used to improve river habitat as part of restoration

efforts, and these findings emphasise the importance of wood structure and positioning for river restoration design.

Acknowledgments

This research was carried out within the Erasmus Mundus Doctorate Program SMART (Science for River Management and their tidal Systems) funded by the Education, Audiovisual and Culture Executive Agency (EACEA) of the European Commission. We are grateful to Ed Oliver in the School of Geography at Queen Mary University of London for help producing the Figures. We thank Marcello Trinci and Marco Dal Molin for their help with fieldwork. The authors have no conflict of interests.

Data availability statement

The data that support the findings of this study are available from the corresponding author upon reasonable request.

List of Tables

Table 1. Variables used to represent the four IPOS categories (intensity, periodicity, orientation, scale) identified by Lacey *et al.* (2012), where x = u, v, w components; N = number of observations; ρ = water density; u', v' and w' are the turbulent residuals; and U, V, W the mean velocities along the three components (streamwise (u), lateral (v) and vertical (w) components). For more info see Table 1 in Trinci *et al.*, 2017. *denotes additional variables to those directly identified in Lacey *et al.*, 2012).

Table 2. Summary statistics of the key IPOS parameters across the two patches. Bold font refers to statistically different (Mann Whitney: $p < 0.001$).

Table 3. Summary of regression model used to predict SI (Selection index) using different sets of predictors. Bold font refers to statistically significant variables ($p < 0.05$).

References

Barber, I., & Wright, H. A. (2001). How strong are familiarity preferences in shoaling fish? Animal Behaviour, 61(5), 975-979.

Benitez, J. P., & Ovidio, M. (2018). The influence of environmental factors on the upstream movements of rheophilic cyprinids according to their position in a river basin. Ecology of Freshwater Fish, 27(3), 660-671.

Brasington, J., & Richards, K. (2000). Turbidity and suspended sediment dynamics in small catchments in the Nepal Middle Hills. Hydrological Processes, 14(14), 2559-2574.

Boisclair, D., & Tang, M. (1993). Empirical analysis of the influence of swimming pattern on the net energetic cost of swimming in fishes. Journal of Fish Biology, 42(2), 169-183.

Blanckaert, K., Kleinhans, M. G., McLelland, S. J., Uijttewaal, W. S., Murphy, B. J., van de Kruijs, A., ... & Chen, Q. (2013). Flow separation at the inner (convex) and outer (concave) banks of constant-width and widening open-channel bends. Earth Surface Processes and Landforms, 38(7), 696-716.

Buffin- Belanger, T. & Roy, A. G. (2005). 1 min in the life of a river: selecting the optimal record length for the measurement of turbulence in fluvial boundary layers. Geomorphology, 68, 77-94.

Cashman, M. J., Pilotto, F., Harvey, G. L., Wharton, G., & Pusch, M. T. (2016). Combined stable isotope and fatty acid analyses demonstrate that large wood increases the autochthonous trophic base of a macroinvertebrate assemblage. Freshwater Biology, 61, 549–564.

Cashman M, Wharton G, Harvey GL, Naura M and Bryden A (2018). Trends in the use of large wood in UK river restoration projects: insights from the National River Restoration Inventory. Water and Environment Journal, 33(3), 318-328.

Chatfield, C. 2004. The analysis of time series: an introduction, Boca Raton, Florida, USA, CRC press LLC.

Clifford, N. J., French, J. R. AND Hardisty, J. (1993). Turbulence: Perspectives on Flow And Sediment Transport, Chichester, UK, John Wiley & Sons Ltd.

Cotel, A. J., Webb, P. W., & Tritico, H. (2006). Do brown trout choose locations with reduced turbulence? Transactions of the American Fisheries Society, 135(3), 610-619.

Cotel, A., & Webb, P. (2015). Living in a Turbulent World—A New Conceptual Framework for the Interactions of Fish and Eddies, Integrative and Comparative Biology, 55(4), 662–672.

Cui, Y., & Wootton, R. J. (1988). The metabolic rate of the minnow, *Phoxinus phoxinus* (L.)(*Pisces: Cyprinidae*), in relation to ration, body size and temperature. Functional Ecology, 2(2), 157-161.

Dean, C. B. (1992). Testing for overdispersion in Poisson and binomial regression models. Journal of the American Statistical Association, 87(418), 451-457.

Delcourt, J., Denoël, M., Ylieff, M., & Poncin, P. (2013). Video multitracking of fish behaviour: a synthesis and future perspectives. Fish and Fisheries, 14(2), 186-204.

Dell, A. I., Bender, J. A., Branson, K., Couzin, I. D., de Polavieja, G. G., Noldus, L. P., ... & Brose, U. (2014). Automated image-based tracking and its application in ecology. Trends in Ecology & Evolution, 29(7), 417-428.

Enders, E. C., Boisclair, D., & Roy, A. G. (2003). The effect of turbulence on the cost of swimming for juvenile Atlantic salmon (*Salmo salar*). Canadian Journal of Fisheries and Aquatic Sciences, 60(9), 1149-1160.

Enders, E. C., Boisclair, D., & Roy, A. G. (2005). A model of total swimming costs in turbulent flow for juvenile Atlantic salmon (*Salmo salar*). Canadian Journal of Fisheries and Aquatic Sciences, 62(5), 1079-1089.

Enders, E. C., & Scruton, D. A. (2006). Potential application of bioenergetics models to habitat modeling and importance of appropriate metabolic rate estimates with special consideration for Atlantic salmon. Science Branch, Canadian Technical Report of Fisheries and Aquatic Science 2641: 1-40.

Enders, E. C., & Boisclair, D. (2016). Effects of environmental fluctuations on fish metabolism: Atlantic salmon *Salmo salar* as a case study. Journal of Fish Biology, 88(1), 344-358.

Fish, F. E. (2010). Swimming strategies for energy economy. Fish swimming: an etho-ecological perspective. Taylor and Francis, Oxford: 90–122.

Froese, R. (1998). Length-weight relationships for 18 less-studied fish species. Journal of Applied Ichthyology, 14(1-2), 117-118.

Goettel, M. T., Atkinson, J. F., & Bennett, S. J. (2015). Behavior of western blacknose dace in a turbulence modified flow field. Ecological Engineering, 74, 230-240.

Goring, D. G., & Nikora, V. I. (2002). Despiking acoustic Doppler velocimeter data. Journal of Hydraulic Engineering, 128(1), 117-126.

Gurnell, A. M., & Sweet, R. (1998). The distribution of large woody debris accumulations and pools in relation to woodland stream management in a small, low-gradient stream. Earth Surface Processes and Landforms: The Journal of the British Geomorphological Group, 23(12), 1101-1121.

Gurnell, A. M., Petts, G. E., Hannah, D. M., Smith, B. P., Edwards, P. J., Kollmann, J., & Tockner, K. (2001). Riparian vegetation and island formation along the gravel-bed Fiume

Tagliamento, Italy. Earth Surface Processes and Landforms: The Journal of the British Geomorphological Research Group, 26(1), 31-62.

Gurnell, A., & Petts, G. (2006). Trees as riparian engineers: the Tagliamento River, Italy. Earth Surface Processes and Landforms: The Journal of the British Geomorphological Research Group, 31(12), 1558-1574.

Gurnell, A. (2014). Plants as river system engineers. Earth Surface Processes and Landforms, 39(1), 4-25.

Hardy, R. J., Best, J. L., Lane, S. N., & Carbonneau, P. E. (2009). Coherent flow structures in a depth-limited flow over a gravel surface: The role of near-bed turbulence and influence of Reynolds number. Journal of Geophysical Research: Earth Surface, 114(F1).

Hart, P. J. (2003). Habitat use and feeding behaviour in two closely related fish species, the three-spined and nine-spined stickleback: an experimental analysis. Journal of Animal Ecology, 72(5), 777-783.

Harvey, G. L., & Clifford, N. J. (2009). Microscale hydrodynamics and coherent flow structures in rivers: implications for the characterization of physical habitat. River Research and Applications, 25(2), 160-180.

Harvey, G. L., Henshaw, A. J., Parker, C., & Sayer, C. D. (2018). Re-introduction of structurally complex wood jams promotes channel and habitat recovery from overwidening: Implications for river conservation. Aquatic Conservation: Marine and Freshwater Ecosystems, 28(2), 395-407.

Higham, T. E., Stewart, W. J., & Wainwright, P. C. (2015). Turbulence, temperature, and turbidity: the ecomechanics of predator–prey interactions in fishes. Integrative and Comparative Biology, 55(1), 6-20.

Hooke, R. L. B. (1975). Distribution of sediment transport and shear stress in a meander bend. The Journal of Geology, 83(5), 543-565.

Hurlbert, S. H. (1984). Pseudoreplication and the design of ecological field experiments. Ecological Monographs, 54(2), 187-211.

Karrenberg, S., Kollmann, J., Edwards, P. J., Gurnell, A. M., & Petts, G. E. (2003). Patterns in woody vegetation along the active zone of a near-natural Alpine river. Basic and Applied Ecology, 4(2), 157-166.

Kemp, P. S., Russon, I. J., Vowles, A. S., & Lucas, M. C. (2011). The influence of discharge and temperature on the ability of upstream migrant adult river lamprey (*Lampetra fluviatilis*) to pass experimental overshot and undershot weirs. River Research and Applications, 27(4), 488-498.

Kottelat, M., & Freyhof, J. (2007). Handbook of European freshwater fishes. Publications Kottelat.

Lacey, R. J., Neary, V. S., Liao, J. C., Enders, E. C., & Tritico, H. M. (2012). The IPOS framework: linking fish swimming performance in altered flows from laboratory experiments to rivers. River Research and Applications, 28(4), 429-443.

Leclerc, M., Boudreault, A., Bechara, T. A., & Corfa, G. (1995). Two-dimensional hydrodynamic modeling: a neglected tool in the instream flow incremental methodology. Transactions of the American Fisheries Society, 124(5), 645-662.

MacVicar, B. J., & Roy, A. G. (2007). Hydrodynamics of a forced riffle pool in a gravel bed river: 1. Mean velocity and turbulence intensity. Water Resources Research, 43(12), 1-17.

Mills, C. A., & Eloranta, A. (1985, January). The biology of *Phoxinus phoxinus* (L.) and other littoral zone fishes in Lake Konnevesi, central Finland. Annales Zoologici Fennici, 22(1), 1-12.

Milne, J. A., & Sear, D. A. (1997). Modelling river channel topography using GIS. International Journal of Geographical Information Science, 11(5), 499-519.

Miranda, R., Oscoz, J., Leunda, P. M., & Escala, M. C. (2006). Weight–length relationships of cyprinid fishes of the Iberian Peninsula. Journal of Applied Ichthyology, 22(4), 297-298.

Morris, D.G., Flavin, R.W., 1990. A digital terrain model for hydrology. In:Proceedings of 4th International Symposium on Spatial Data Handling, Zurich(CH), pp. 250–262.

Neuswanger, J. R., Wipfli, M. S., Rosenberger, A. E., & Hughes, N. F. (2016). Measuring fish and their physical habitats: versatile 2D and 3D video techniques with user-friendly software. Canadian Journal of Fisheries and Aquatic Sciences, 73(12), 1861-1873.

Nikora, V. I., & Goring, D. G. (1998). ADV measurements of turbulence: Can we improve their interpretation? Journal of Hydraulic Engineering, 124(6), 630-634.

Oscoz, J., Campos, F., & Escala, M. C. (2005). Weight–length relationships of some fish species of the Iberian Peninsula. Journal of Applied Ichthyology, 21(1), 73-74.

Pilotto, F., Bertoncin, A., Harvey, G. L., Wharton, G., & Pusch, M. T. (2014). Diversification of stream invertebrate communities by large wood. Freshwater Biology, 59(12), 2571-2583.

Preece, J. (2017). How two billion smartphone users can save species! Interactions, 24(2), 26-33.

Pitcher, T. J. (1986). Functions of shoaling behaviour in teleosts. In: The Behavior of Teleost Fishes (Pitcher, T. J. ed.), pp. 363–439. London: Chapman & Hall.

Plath, M., Sarbu, A., Erkoc, K., Bierbach, D., Jourdan, J., & Schleucher, E. (2013). Energetic costs of group-living? A reversed “group effect” in shoaling minnows (*Phoxinus phoxinus*). Bulletin of Fish Biology, 14, 1-10.

Rifflart, R., Carrel, G., Le Coarer, Y., & FONTEZ, B. N. T. (2009). Spatio-temporal patterns of fish assemblages in a large regulated alluvial river. Freshwater Biology, 54(7), 1544-1559.

Rusello, P. J., Lohrmann, A., Siegel, E., & Maddux, T. (2006). Improvements in acoustic Doppler velocimetery. In The 7th Int. Conf. in Hydroscience and Engineering (ICHE 2006), 10–13 September, Philadelphia, PA, USA. Philadelphia, PA: Michael Piasecki/College of Engineering, Drexel University.

Schneider, K. N., & Winemiller, K. O. (2008). Structural complexity of woody debris patches influences fish and macroinvertebrate species richness in a temperate floodplain-river system. Hydrobiologia, 610(1), 235-244.

Silva, A. T., Santos, J. M., Ferreira, M. T., Pinheiro, A. N., & Katopodis, C. (2011). Effects of water velocity and turbulence on the behaviour of Iberian barbel (*Luciobarbus bocagei*, Steindachner 1864) in an experimental pool-type fishway. River Research and Applications, 27(3), 360-373.

Simonović, P. D., Garner, P., Eastwood, E. A., Kováč, V., & Copp, G. H. (1999). Correspondence between ontogenetic shifts in morphology and habitat use in minnow *Phoxinus phoxinus*. Environmental Biology of Fishes, 56(1-2), 117-128.

Silva, A. T., Katopodis, C., Santos, J. M., Ferreira, M. T., & Pinheiro, A. N. (2012). Cyprinid swimming behaviour in response to turbulent flow. Ecological Engineering, 44, 314-328.

Spampinato, C., Chen-Burger, Y. H., Nadarajan, G., & Fisher, R. B. (2008). Detecting, Tracking and Counting Fish in Low Quality Unconstrained Underwater Videos. Vision Theory and Application (2), 514-519.

Spampinato, C., Giordano, D., Di Salvo, R., Chen-Burger, Y. H. J., Fisher, R. B., & Nadarajan, G. (2010). Automatic fish classification for underwater species behavior understanding. In

Proceedings of the first ACM international workshop on Analysis and retrieval of tracked events and motion in imagery streams, 45-50.

Sukhodolov, A. N., & Sukhodolova, T. A. (2014). Shallow wake behind exposed wood-induced bar in a gravel-bed river. Environmental Fluid Mechanics, 14(5), 1071-1083.

Tiffan, K. F., Haskell, C. A., & Kock, T. J. (2010). Quantifying the behavioral response of spawning chum salmon to elevated discharges from Bonneville Dam, Columbia river, USA. River Research and Applications, 26(2), 87-101.

Trinci, G., Harvey, G. L., Henshaw, A. J., Bertoldi, W., & Hölker, F. (2017). Life in turbulent flows: interactions between hydrodynamics and aquatic organisms in rivers. Wiley Interdisciplinary Reviews: Water, 4(3), e1213.

Trinci, G. (2017). Spatial organization of ecologically-relevant high order flow properties and implications for river habitat assessment (Doctoral dissertation, Queen Mary University of London and University of Trento).

Tritico, H. M., & Cotel, A. J. (2010). The effects of turbulent eddies on the stability and critical swimming speed of creek chub (*Semotilus atromaculatus*). Journal of Experimental Biology, 213(13), 2284-2293.

Tullos, D., & Walter, C. (2015). Fish use of turbulence around wood in winter: physical experiments on hydraulic variability and habitat selection by juvenile coho salmon, *Oncorhynchus kisutch*. Environmental Biology of Fishes, 98(5), 1339-1353.

Tullos, D., Walter, C., & Dunham, J. (2016). Does resolution of flow field observation influence apparent habitat use and energy expenditure in juvenile coho salmon? Water Resources Research, 52(8), 5938-5950.

Vogel, S. 1994. Life in moving fluids: the physical biology of flow, Princeton University Press.

Ward, J. V., Tockner, K., Edwards, P. J., Kollmann, J., Bretschko, G., Gurnell, A. M., ... & Rossaro, B. (1999). A reference river system for the Alps: the 'Fiume Tagliamento'. River Research and Applications, 15(1-3), 63-75.

Ward, J. V., & Tockner, K. (2001). Biodiversity: towards a unifying theme for river ecology. Freshwater Biology, 46(6), 807-820.

Ward, A. J., & Krause, J. (2001). Body length assortative shoaling in the European minnow, *Phoxinus phoxinus*. Animal Behaviour, 62(4), 617-621.

Webb, P. W., Kostecki, P. T., & Stevens, E. D. (1984). The effect of size and swimming speed on locomotor kinematics of rainbow trout. Journal of Experimental Biology, 109(1), 77-95.

Webb, P. W. (1988). Simple physical principles and vertebrate aquatic locomotion. American Zoologist, 28(2), 709-725.

Webb, P. W., & Cotel, A. J. (2010). Turbulence: does vorticity affect the structure and shape of body and fin propulsors? Integrative and comparative Biology, 50(6), 1155-1166.

Wilcox, A. C., & Wohl, E. E. (2007). Field measurements of three-dimensional hydraulics in a step-pool channel. Geomorphology, 83(3-4), 215-231.

Wilkes, M. A., Maddock, I., Visser, F., & Acreman, M. C. (2013). Incorporating hydrodynamics into Ecohydraulics: The Role of Turbulence in the Swimming Performance and Habitat Selection of Stream-Dwelling Fish. Ecohydraulics: an integrated approach, 7-30.

Wilkes, M. A., Enders, E. C., Silva, A. T., Acreman, M., & Maddock, I. 2017. Position choice and swimming costs of juvenile Atlantic salmon *Salmo salar* in turbulent flow. Journal of Ecohydraulics, 2(1), 16-27.

Wohl, E. (2017). Bridging the gaps: An overview of wood across time and space in diverse rivers. Geomorphology, 279, 3-26.

Zika, U., & Peter, A. (2002). The introduction of woody debris into a channelized stream: effect on trout populations and habitat. River Research and Applications, 18(4), 355-366.

Zhou, C., Xu, D., Lin, K., Sun, C., & Yang, X. (2018). Intelligent feeding control methods in aquaculture with an emphasis on fish: a review. Reviews in Aquaculture, 10(4), 975-993.

Table 1. Variables used to represent the four IPOS categories (intensity, periodicity, orientation, scale) identified by Lacey *et al.* (2012), where x = u, v, w components; N = number of observations; ρ = water density; u', v' and w' are the turbulent residuals; and U, V, W the mean velocities along the three components (streamwise (u), lateral (v) and vertical (w) components). For more info see Table 1 in Trinci *et al.,* 2017. *denotes additional variables to those directly identified in Lacey *et al*. 2012).

	Parameter	**Formula**
Intensity	Turbulence intensity (absolute) (ms^{-1})	$RMS_x = \sqrt{\frac{1}{N}\left(x'^2_1 + x'^2_2 + \cdots + x'^2_N\right)}$
	Turbulence intensity (relative)	$TI_x = \frac{\sigma_x}{U}$
	TKE (m^2s^{-2})	$TKE = \frac{1}{2}\rho(RMS_x^2 + RMS_x^2 + RMS_x^2)$
	Reynolds shear stress (Nm^2)	$\tau_{uv} = \rho\overline{u'v'}\ \ \tau_{uw} = \rho\overline{u'w'}\ \ \tau_{vw} = \rho\overline{v'w'}$
	Vorticity (speed of the fluid) (s^{-1})	$\omega = 2\Omega$ Where Ω represents the angular velocity.
Periodicity	Kurtosis*	$K = \frac{\sum_1^N \left(\frac{x_i - \bar{x}}{\sigma}\right)^4}{N}$
	AR(2) models applied and the condition for pseudo-periodicity* derived.	$ITS_{u,v,w} = \int_0^\infty R(t)dt$ (where R(t) is the normalized autocorrelation function and t is the time lag).

Orientation	Skewness*	$K = \frac{\sum_1^N \left(\frac{x_i - \bar{x}}{\sigma}\right)^3}{N}$
	Event Structure*	Duration and/or contribution to stress of each type of 'event': Q1 (u'>0, w'>0; outward interactions), Q2 (u'<0, w'>0; ejections of fluid away from the bed), Q3 (u'<0, w'<0; inward interactions) and Q4 (u'>0, w'<0; inrushes of fluid towards the bed).
Scale	Eddy length scale (m)	L=Ut Where L represents an average eddy length using mean velocity (U) and t (time).
	Length-scale ratio*	$\frac{Wedge\ momentum}{Fish\ momentum} = \frac{L_u * u_e}{L_f * u_f}$ Where Lu is the length scale and Lf fish length and u_e convection velocity of the wedge and u_f fish velocity :
	Eddy diameter (m)	Spatial extent of rotating fluid.

Table 2. Summary statistics of the key IPOS parameters across the two patches. Bold font refers to statistically different (Mann Whitney: $p < 0.001$).

		Patch 1		Patch 2	
	Variables	**Mean**	**SD**	**Mean**	**SD**
Mean velocity	**U (m s^{-1})**	-0.11	0.044	0.18	0.112
	V (m s^{-1})	0.08	0.015	0.03	0.036
	W (m s^{-1})	-0.01	0.036	-0.02	0.032
Intensity	TKE (m^2 s^{-2})	0.04	0.012	0.03	0.012
	Reuv (N m^{-2})	2.34	1.412	1.65	1.398
	Reuw (N m^{-2})	1.53	1.277	0.97	0.860
	Vorticity (s^{-1})	0.11	0.041	0.19	0.101
Orientation	%Q1	0.29	0.305	0.29	0.215
	%Q2	0.32	0.269	0.22	0.109
	%Q3	0.06	0.044	0.223	0.156
	%Q4	0.35	0.333	0.26	0.188
Predictability	Pseudo -period. u	-1.65	1.272	-0.47	0.422
	Pseudo -period. v	-1.49	1.121	-0.33	0.801
	Pseudo -period. w	-0.93	1.036	0.11	0.715
Scale	Lu (m)	0.17	0.089	0.21	0.068
	Lv (m)	0.12	0.034	0.05	0.051

	Lw (m)	0.04	0.022	0.02	0.015
	Du (m)	0.037	0.017	0.031	0.013
	Dv (m)	0.006	0.004	0.026	0.002
	Dw (m)	0.003	0.002	0.005	0.004

Table 3. Summary of regression model used to predict SI (Selection index) using different sets of predictors. Bold font refers to statistically significant variables ($p < 0.05$).

Predictor	**B (Coefficient)**	**SE**	**Wald |Chi square**	**p**
Intercept	4.6	0.3	220.2	**0.000**
SC_1	-0.5	0.2	6.5	**0.011**
PC1	-0.2	0.2	6.8	**0.009**
PC2	-0.0	0.2	1.1	0.855
PC3	-0.6	0.1	10.5	**0.001**
Resultant Velocity	-0.9	4.33	0.2	0.640